Thermal noise and dephasing due to electron interactions in nontrivial geometries

M. Treiber,[1] C. Texier,[2] O. M. Yevtushenko,[1] J. von Delft,[1] and I. V. Lerner[3]

[1]*Ludwig Maximilians University, Arnold Sommerfeld Center and Center for Nano-Science, Munich, DE-80333, Germany*

[2]*Univ. Paris Sud, CNRS, LPTMS, UMR 8626 & LPS, UMR 8502, Orsay FR-91405, France*

[3]*School of Physics and Astronomy, University of Birmingham, Birmingham, B15 2TT, United Kingdom*

(Received 5 May 2011; published 5 August 2011)

We study Johnson-Nyquist noise in macroscopically inhomogeneous disordered metals and give a microscopic derivation of the correlation function of the scalar electric potentials in real space. Starting from the interacting Hamiltonian for electrons in a metal and the random phase approximation, we find a relation between the correlation function of the electric potentials and the density fluctuations, which is valid for arbitrary geometry and dimensionality. We show that the potential fluctuations are proportional to the solution of the diffusion equation, taken at zero frequency. As an example, we consider networks of quasi-one-dimensional disordered wires and give an explicit expression for the correlation function in a ring attached via arms to absorbing leads. We use this result in order to develop a theory of dephasing by electronic noise in multiply-connected systems.

DOI: 10.1103/PhysRevB.84.054204 PACS number(s): 07.50.Hp, 42.50.Lc, 73.63.−b

I. INTRODUCTION

Electronic noise generated by the thermal excitation of charge carriers has been observed and explained by Johnson and Nyquist more than 80 years ago[1] and discussed in great detail in the literature since then. More recently, it has been found that this so-called Johnson-Nyquist noise is the main source of dephasing in mesoscopic systems at low temperatures of a few Kelvins where phonons are frozen out. Dephasing puts an IR cut-off for interference phenomena, such as quantum corrections to the classical conductivity.[2]

The current interest in this topic arises from studies of dephasing in mesoscopic systems which consist of connected quasi-one-dimensional (1D) disordered wires, see Fig. 1, including connected rings and grids.[3,4] It has been found (both experimentally[5] and theoretically[6–10]) that dephasing depends not only on the dimensionality, but also on the geometry of the system. The noise correlation function is well-understood for macroscopically homogeneous systems such as infinite wires or isolated rings, but has so-far not been studied in multiply-connected networks with leads attached at arbitrary points. The goal of this paper is to give a transparent and systematic description of the thermal noise properties for such systems. In particular, we will derive an expression for the fluctuations of the scalar electric potentials for arbitrary geometries, Eq. (31), and a general expression for the corresponding dephasing rate, Eq. (45). Throughout, we assume that a description of the noise in terms of scalar potentials is sufficient, i.e., we neglect the fluctuations of the transverse component of the electromagnetic field (for a detailed discussion of the latter, see Ref. 2).

Let us start by reviewing simplified arguments to derive the noise correlation function: Johnson and Nyquist concluded that thermal noise in electrical conductors is approximately white, meaning that the power spectral density is nearly constant throughout the whole frequency spectrum. If, in addition, the fluctuations are uncorrelated for different points in space, a correlation function for the random thermal currents in the classical limit is independent of frequency ω and momentum $\boldsymbol{q}$. The power spectrum of the current density reads

$$\langle|\boldsymbol{j}|^2\rangle(\boldsymbol{q},\omega) = 2T\sigma_0\,. \tag{1}$$

Here, $\sigma_0 = e^2\nu D$ is the Drude conductivity of the disordered system, D and ν are the diffusion constant and the density of states, respectively. Naively applying Ohm's law, $\boldsymbol{j}(\boldsymbol{q}) = \sigma_0\boldsymbol{E}(\boldsymbol{q})$, to Eq. (1) and using the relation between the electric field and the scalar potential, $e\boldsymbol{E}(\boldsymbol{q}) = -i\boldsymbol{q}V(\boldsymbol{q})$, we find

$$\langle|V|^2\rangle(\boldsymbol{q},\omega) = \frac{2Te^2}{\sigma_0}\frac{1}{\boldsymbol{q}^2}\,. \tag{2}$$

The correlation function, Eq. (2), corresponds to the coupling of a given electron to the bath of the surrounding electrons.[2] Thus $\langle|V|^2\rangle$ describes the process of successive emission and reabsorption of a photon, which is described effectively by the scalar potential V. The factor $1/\boldsymbol{q}^2$ coincides with the solution of a diffusion equation in an infinite system, which reflects the fact that the currents, Eq. (1), are uncorrelated in space.

These simple arguments are based on the homogeneity of the system and have assumed a local relation between potential and current, whereas transport properties in disordered metals are substantially nonlocal.[10–13] In this paper, we derive an analogy of Eq. (2) for disordered systems with arbitrary geometry and dimensionality; this will in particular apply to networks of disordered wires. A detailed calculation, which takes into account all properties of the mesoscopic samples, has to be done in the real-space representation. Starting points are the usual linear response formalism and the fluctuation-dissipation theorem (FDT).[14] Although most ingredients of the following discussion will be familiar to experts, we hope that the manner in which they have been assembled here will be found not only to be pedagogically useful, but also helpful for further theoretical studies.

The paper is organized as follows: in Sec. II, we propose a heuristic description of the potential fluctuations. In Sec. III, we review a microscopic approach to the noise correlation function, based on a relation of the fluctuations of the scalar potentials to the fluctuations of the density, using the random phase approximation (RPA). In Sec. IV, we evaluate the density response function χ for disordered systems by using a real-space representation for arbitrary geometries. We apply this result to the noise correlation function in Sec. V. In Sec. VI, we show how the noise correlation function can be calculated for networks of disordered wires. Finally, in Sec. VII, we

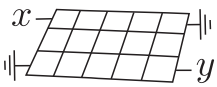

FIG. 1. A network of wires. We are interested in the noise correlations between arbitrary points $\boldsymbol{x}$ and $\boldsymbol{y}$ of multiply-connected networks attached to leads (denoted by the usual ground symbol) at arbitrary points.

discuss the relation to the fundamental problem of dephasing by electronic interactions.

II. HEURISTIC DESCRIPTION OF POTENTIAL FLUCTUATIONS

A description of fluctuations in metals within the linear response formalism naturally starts with an analysis of the density fluctuations in the model of noninteracting electrons described by the standard free-electron Hamiltonian $\hat{H}^{(0)}$. This system is perturbed by an external scalar potential $V(\boldsymbol{x},t)$ coupled to the density operator $\hat{n}(\boldsymbol{x})$:

$$\hat{H}^{(1)} = \int d\boldsymbol{x}\, V(\boldsymbol{x},t)\,\hat{n}(\boldsymbol{x})\,. \tag{3}$$

The response of the (induced) charge density,

$$\begin{aligned} n_{\rm ind}(\boldsymbol{x},\omega) &\equiv \int_{-\infty}^{\infty} dt\, e^{i\omega t}[\langle \hat{n}(\boldsymbol{x},t)\rangle_{\rm pert} - \langle \hat{n}(\boldsymbol{x})\rangle] \\ &= -\int d\boldsymbol{y}\, \chi(\boldsymbol{x},\boldsymbol{y},\omega)\, V(\boldsymbol{y},\omega)\,, \end{aligned} \tag{4}$$

is governed by the (retarded) density response function:

$$\chi(\boldsymbol{x},\boldsymbol{y},\omega) = i\int_0^{\infty} dt\, e^{i(\omega+i0)t}\langle[\hat{n}(\boldsymbol{x},t),\hat{n}(\boldsymbol{y},0)]\rangle\,. \tag{5}$$

Here, $\langle\cdots\rangle_{\rm pert}$ and $\langle\cdots\rangle$ denote quantum/statistical averaging with respect to the perturbed and unperturbed Hamiltonian, respectively. The FDT relates the equilibrium density fluctuations to the imaginary (dissipative) part of the response function,

$$\langle|n|^2\rangle(\boldsymbol{x},\boldsymbol{y},\omega) \equiv \int_{-\infty}^{\infty} dt\, e^{i\omega t}\,\langle \hat{n}(\boldsymbol{x},t)\,\hat{n}(\boldsymbol{y},0)\rangle \tag{6}$$

$$= F(\omega)\,{\rm Im}[\chi(\boldsymbol{x},\boldsymbol{y},\omega)]\,, \tag{7}$$

where

$$F(\omega) = \frac{2}{1-e^{-\omega/T}}\,. \tag{8}$$

In writing Eqs. (6)–(8), we have exploited detailed balance and time-reversal symmetry. The latter implies $\chi(\boldsymbol{x},\boldsymbol{y},\omega) = \chi(\boldsymbol{y},\boldsymbol{x},\omega)$.[14]

The question, which we are going to address in this paper, is how to characterize the fluctuations of the electric potential V. For this purpose we consider the "dual" case, where some external density $n_{\rm ext}(\boldsymbol{x},t)$ is the perturbation that couples to the "potential operator" $\hat{V}$:[15]

$$\hat{H}^{(2)} = \int d\boldsymbol{x}\, \hat{V}(\boldsymbol{x})\, n_{\rm ext}(\boldsymbol{x},t)\,. \tag{9}$$

The linear response of $\hat{V}$ to the perturbation can be written as

$$\langle \hat{V}(\boldsymbol{x},\omega)\rangle_{\rm pert} = \int d\boldsymbol{y}\, \Upsilon(\boldsymbol{x},\boldsymbol{y},\omega)\, n_{\rm ext}(\boldsymbol{y},\omega)\,, \tag{10}$$

defining the response function Υ. In analogy to Eq. (7), the response function also characterizes the equilibrium fluctuations of the potential:[16]

$$\langle|V|^2\rangle(\boldsymbol{x},\boldsymbol{y},\omega) = F(\omega)\,{\rm Im}[-\Upsilon(\boldsymbol{x},\boldsymbol{y},\omega)]\,. \tag{11}$$

Calculating the response function $\Upsilon(\boldsymbol{x},\boldsymbol{y},\omega)$ is a complicated task because it requires precise knowledge of the potential operator $\hat{V}(\boldsymbol{x})$. Instead, we can identify the potential $V(\boldsymbol{x},\omega)$ in Eq. (4) with the response $\langle \hat{V}(\boldsymbol{x},\omega)\rangle_{\rm pert}$ in Eq. (10) to relate Υ to χ: in the limit of strong screening in good conductors (called the unitary limit[9]), electroneutrality is satisfied locally. Therefore, the induced charge exactly compensates the external charge: $n_{\rm ind}(\boldsymbol{x},\omega) = -n_{\rm ext}(\boldsymbol{x},\omega)$. Now inserting Eq. (4) into Eq. (10) (or vice versa), we obtain

$$\int d\boldsymbol{x}'\,\Upsilon(\boldsymbol{x},\boldsymbol{x}',\omega)\chi(\boldsymbol{x}',\boldsymbol{y},\omega) = \delta(\boldsymbol{x}-\boldsymbol{y})\,. \tag{12}$$

If χ is known, Eqs. (11) and (12) allow one to calculate the correlation function of the scalar potential.

Let us recall the well-known case of macroscopically homogeneous diffusive systems. The expression for the disordered averaged response function $\overline{\chi}$ reads[17,18]

$$\overline{\chi}(\boldsymbol{q},\omega) = \nu\frac{D\boldsymbol{q}^2}{D\boldsymbol{q}^2 - i\omega} = 1/\Upsilon(\boldsymbol{q},\omega)\,, \tag{13}$$

where we used Eq. (12). Inserting Eq. (13) into Eq. (11), we find

$$\langle|V|^2\rangle(\boldsymbol{q},\omega) = \frac{1}{\nu}\frac{\omega F(\omega)}{D\boldsymbol{q}^2}\,, \tag{14}$$

which reduces to Eq. (2) in the limit $\omega \ll T$.

III. NOISE CORRELATION FUNCTION FOR ARBITRARY GEOMETRIES: MICROSCOPIC APPROACH

In Eqs. (3) and (9), we introduced the operators $\hat{n}$ and $\hat{V}$ assuming that either $V(\boldsymbol{x},t)$ or $n_{\rm ext}(\boldsymbol{x},t)$ are external perturbations. In fact, the fluctuations originate inside of the system and the starting point of a microscopic description is the part of the Hamiltonian, which describes electron interactions,

$$\hat{H}_{\rm int} = \int d\boldsymbol{x}d\boldsymbol{y}\, U_0(\boldsymbol{x},\boldsymbol{y})\hat{\psi}^{\dagger}(\boldsymbol{x})\hat{\psi}^{\dagger}(\boldsymbol{y})\hat{\psi}(\boldsymbol{y})\hat{\psi}(\boldsymbol{x})\,, \tag{15}$$

where $U_0(\boldsymbol{x},\boldsymbol{y})$ is the bare Coulomb interaction. In the mean-field approximation, Eq. (15) gives rise to a correction, called Hartree contribution, to the electron energy:

$$\Delta E^{\rm (Hartree)} \approx \int d\boldsymbol{x}d\boldsymbol{y}\, U_0(\boldsymbol{x},\boldsymbol{y})\langle\hat{n}(\boldsymbol{x})\rangle\langle\hat{n}(\boldsymbol{y})\rangle\,, \tag{16}$$

where $\hat{n}(\boldsymbol{x}) = \hat{\psi}^{\dagger}(\boldsymbol{x})\hat{\psi}(\boldsymbol{x})$.

The Coulomb interactions are dynamically screened, which can be accounted for in the framework of the RPA, provided that the electron density is high,

$$\begin{aligned} U_{\rm RPA}(\boldsymbol{x},\boldsymbol{y},\omega) = U_0(\boldsymbol{x},\boldsymbol{y}) &- \int d\boldsymbol{x}'d\boldsymbol{y}' U_0(\boldsymbol{x},\boldsymbol{x}')\chi(\boldsymbol{x}',\boldsymbol{y}',\omega) \\ &\times U_{\rm RPA}(\boldsymbol{y}',\boldsymbol{y},\omega)\,, \end{aligned} \tag{17}$$

see Fig. 2. Note that $-\chi$ [see the definition in Eq. (5)] is equal to the bubble diagrams of Fig. 2, see e.g., Ref. 18. In

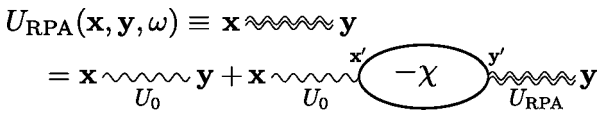

FIG. 2. The Coulomb interaction in the RPA according to Eq. (17).

Appendix A, we recall how to obtain Eq. (17) within a self-consistent treatment of the screening problem.

Using the RPA in Eq. (16) and comparing the result with equation Eq. (9), we observe that the potential fluctuations are due to electronic interactions and that the operator of the scalar potential is given by

$$\hat{V}(\boldsymbol{x},\omega) = \int d\boldsymbol{y}\, U_{\rm RPA}(\boldsymbol{x},\boldsymbol{y},\omega)\,\hat{n}(\boldsymbol{y})\,. \tag{18}$$

Equation (18) allows us to relate the correlation function of the potentials to the correlation function of the density fluctuations:

$$\langle |V|^2\rangle(\boldsymbol{x},\boldsymbol{y},\omega) = \int d\boldsymbol{x}' d\boldsymbol{y}' U_{\rm RPA}(\boldsymbol{x},\boldsymbol{x}',\omega) \times \langle |n|^2\rangle(\boldsymbol{x}',\boldsymbol{y}',\omega) U^*_{\rm RPA}(\boldsymbol{y}',\boldsymbol{y},\omega)\,. \tag{19}$$

By inserting Eqs. (17) and (7) into Eq. (19), reordering the terms in the RPA series and using the fact that U_0 is real, we find (see Fig. 3)

$$\langle |V|^2\rangle(\boldsymbol{x},\boldsymbol{y},\omega) = F(\omega)\,{\rm Im}[-U_{\rm RPA}(\boldsymbol{x},\boldsymbol{y},\omega)]\,. \tag{20}$$

We emphasize that the derivation of Eq. (20) has not used any other assumption than the RPA. Thus Eqs. (17) and (20) are a microscopic (and more rigorous) counterpart of the phenomenological Eqs. (11) and (12).

IV. DENSITY RESPONSE IN DISORDERED SYSTEMS: CALCULATIONS IN COORDINATE REPRESENTATION

In disordered metals, the motion of the electrons is diffusive, provided that $k_F^{-1} \ll \ell \ll L$, where k_F is the Fermi wave vector, ℓ the mean free path and L the system size. It can be accounted for by substituting the disorder-averaged density response function $\overline{\chi}$, into the phenomenological Eqs. (11)

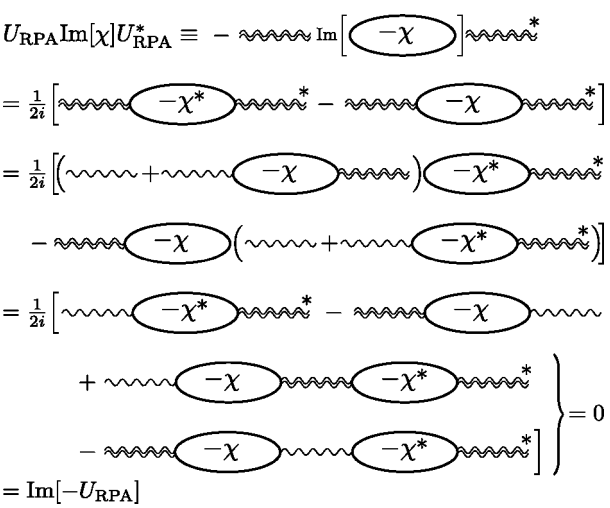

FIG. 3. Diagrammatic proof of Eq. (20) by using Eqs. (17)–(19) (i.e., Fig. 2).

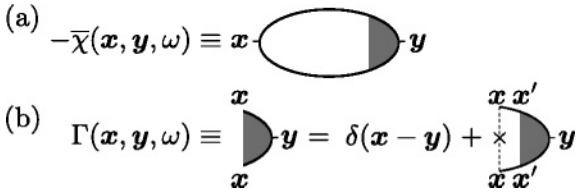

FIG. 4. (a) Equation for the disorder-averaged density response function; solid lines denote the disorder-averaged retarded and/or advanced Green functions, cf. Eq. (21). (b) Equation for the impurity vertex; the dashed line represents impurity scattering, cf. Eq. (23).

and (12) or the microscopic Eqs. (17) and (20). The function $\overline{\chi}$ has been calculated for macroscopically homogeneous systems by Vollhardt and Wölfle.[17] In the following, we will show how to generalize their calculation to inhomogeneous systems. A useful starting point is a coordinate representation of the density response function, Eq. (5), in terms of the advanced and retarded Green's functions $G^{R/A}(\boldsymbol{x},\boldsymbol{y},\omega)$,

$$\begin{aligned}\overline{\chi}(\boldsymbol{x},\boldsymbol{y},\omega) = \frac{1}{2\pi i}\int d\epsilon\,[f(\epsilon+\omega) - f(\epsilon)] \\ \times \overline{(G^R(\boldsymbol{x},\boldsymbol{y},\epsilon+\omega)G^A(\boldsymbol{y},\boldsymbol{x},\epsilon)} \\ + f(\epsilon)\overline{G^R(\boldsymbol{x},\boldsymbol{y},\epsilon+\omega)G^R(\boldsymbol{y},\boldsymbol{x},\epsilon)} \\ - f(\epsilon+\omega)\overline{G^A(\boldsymbol{x},\boldsymbol{y},\epsilon+\omega)G^A(\boldsymbol{y},\boldsymbol{x},\epsilon)})\,,\end{aligned} \tag{21}$$

see Fig. 4(a). Here, $f(\omega)$ is the Fermi distribution function and $\overline{\cdots}$ denotes disorder averaging. The combinations $\overline{G^RG^R}$ and $\overline{G^AG^A}$ give short-range contributions, since the average of the products decouple, e.g., $\overline{G^RG^R} \simeq \overline{G^R}\cdot\overline{G^R} + \mathcal{O}(1/k_F\ell)$, and the disorder averaged Green's functions $\overline{G^R}$ and $\overline{G^A}$ decay on the scale $\ell \ll L$. We will consider contributions to the thermal noise, which are governed by distances larger than ℓ, cf. Ref. 2. Therefore, details of the behavior on short scales are not important for our purposes and we replace the short-range contributions $\overline{G^RG^R}$ and $\overline{G^AG^A}$ by a delta function. The long range contributions $\overline{G^RG^A}$ can be calculated by standard methods,[18]

$$\begin{aligned}\overline{G^R(\boldsymbol{x},\boldsymbol{y},\epsilon+\omega)G^A(\boldsymbol{y},\boldsymbol{x},\epsilon)} = \int d\boldsymbol{x}'\,\overline{G^R}(\boldsymbol{x},\boldsymbol{x}',\epsilon+\omega) \\ \times \overline{G^A}(\boldsymbol{x}',\boldsymbol{x},\epsilon)\Gamma(\boldsymbol{x}',\boldsymbol{y},\omega),\end{aligned} \tag{22}$$

where $\Gamma(\boldsymbol{x},\boldsymbol{y},\omega)$ is the impurity vertex function,

$$\begin{aligned}\Gamma(\boldsymbol{x},\boldsymbol{y},\omega) = \delta(\boldsymbol{x}-\boldsymbol{y}) + \frac{1}{2\pi\nu\tau}\int d\boldsymbol{x}'\,\overline{G^R}(\boldsymbol{x},\boldsymbol{x}',\epsilon+\omega) \\ \times \overline{G^A}(\boldsymbol{x}',\boldsymbol{x},\epsilon)\Gamma(\boldsymbol{x}',\boldsymbol{y},\omega)\end{aligned} \tag{23}$$

(the factor $1/2\pi\nu\tau$, where $\tau = \ell/v_F$ is the transport time, originates from the impurity line), see Fig. 4(b). The short-ranged product $\overline{G^R}\cdot\overline{G^A}$ can be expanded as $\overline{G^R}\cdot\overline{G^A} \simeq 2\pi\nu\tau\,\delta(\boldsymbol{x}-\boldsymbol{x}')[1 + i\omega\tau + \tau D\Delta_x]$, which is obtained by transforming the product to momentum space and expanding in the transferred momentum $\boldsymbol{q}$ and frequency ω, realizing that terms of order $\boldsymbol{q}$ vanish due to symmetry. As a result, Eq. (23) reduces to a diffusion equation:

$$(-i\omega - D\Delta_x)\,\Gamma(\boldsymbol{x},\boldsymbol{y},\omega) = \frac{1}{\tau}\delta(\boldsymbol{x}-\boldsymbol{y}), \tag{24}$$

where $D = v_F \ell/d$ is the diffusion constant for a d dimensional system. Thus, the vertex function is proportional to the diffusion propagator, $\Gamma(\boldsymbol{x},\boldsymbol{y},\omega) = P(\boldsymbol{x},\boldsymbol{y},\omega)/\tau$.

Collecting the short- and long-range contributions and taking the limit $T \ll \epsilon_F$, we obtain from Eq. (21)

$$\overline{\chi}(\boldsymbol{x},\boldsymbol{y},\omega) = \nu\left(\delta(\boldsymbol{x}-\boldsymbol{y}) + i\omega P(\boldsymbol{x},\boldsymbol{y},\omega)\right). \tag{25}$$

Equation (25) is valid for arbitrary geometries since it is based only on the diffusive approximation and does not require macroscopic homogeneity.

V. NOISE CORRELATION FUNCTION IN DISORDERED SYSTEMS

Let us simplify Eq. (17) for a disordered conductor. Using Eq. (25) and

$$-\frac{1}{4\pi e^2}\Delta_x U_0(\boldsymbol{x},\boldsymbol{x}') = \delta(\boldsymbol{x}-\boldsymbol{x}'), \tag{26}$$

Eq. (17) can be written as

$$\left(1-\frac{\Delta_x}{\kappa^2}\right) U_{\mathrm{RPA}}(\boldsymbol{x},\boldsymbol{y},\omega) + i\omega\int d\boldsymbol{x}'\, P(\boldsymbol{x},\boldsymbol{x}',\omega) \times U_{\mathrm{RPA}}(\boldsymbol{x}',\boldsymbol{y},\omega) = \frac{1}{\nu}\delta(\boldsymbol{x}-\boldsymbol{y}), \tag{27}$$

where we introduced the Thomas-Fermi screening wave vector $\kappa = \sqrt{4\pi e^2 \nu}$, which corresponds to the inverse screening length in three dimensional (3D) bulk systems. The kernel of Eq. (27) is a solution to the diffusion equation (24), which can be expanded in terms of eigenfunctions of the Laplace operator. Consequently, the kernel is always separable and Eq. (27) has a unique solution (see, e.g., Ref. 19 for details on how the solution can be found). Using the semigroup property of the diffusion propagators,

$$\int d\boldsymbol{x}'\, P(\boldsymbol{x},\boldsymbol{x}',\omega)P(\boldsymbol{x}',\boldsymbol{y},0) = \frac{i}{\omega}\left[P(\boldsymbol{x},\boldsymbol{y},0) - P(\boldsymbol{x},\boldsymbol{y},\omega)\right],$$

one can check that

$$U_{\mathrm{RPA}}(\boldsymbol{x},\boldsymbol{y},\omega) = \frac{1}{\nu}\left(\frac{1}{-D\Delta_x - i\omega} + \frac{1}{D\kappa^2}\right)^{-1} P(\boldsymbol{x},\boldsymbol{y},0) \tag{28}$$

satisfies Eq. (27). In practice, the 3D Thomas-Fermi screening length κ^{-1} is a microscopic scale, thus the typical value of the first term of the right-hand side of Eq. (28), $(D\boldsymbol{q}_{\mathrm{typ}}^2 - i\omega_{\mathrm{typ}})^{-1}$, is larger than $1/D\kappa^2 = 1/4\pi\sigma_0$ for good conductors (this is the so-called unitary limit, for details see Ref. 9):

$$\frac{1}{|D\boldsymbol{q}_{\mathrm{typ}}^2 - i\omega_{\mathrm{typ}}|} \gg \frac{1}{D\kappa^2}. \tag{29}$$

In this limit, using the diffusion Eq. (24), we obtain from Eq. (28):

$$U_{\mathrm{RPA}}(\boldsymbol{x},\boldsymbol{y},\omega) = \frac{1}{\nu}[\delta(\boldsymbol{x}-\boldsymbol{y}) - i\omega P(\boldsymbol{x},\boldsymbol{y},0)]. \tag{30}$$

We remind that $P(\boldsymbol{x},\boldsymbol{y},0)$ is always real. As a result, Eqs. (20) and (30) yield

$$\langle|V|^2\rangle(\boldsymbol{x},\boldsymbol{y},\omega) = \frac{1}{\nu}\,\omega F(\omega) P(\boldsymbol{x},\boldsymbol{y},0), \tag{31}$$

where $F(\omega)$ is given by Eq. (8). The real-space demonstration of Eqs. (30) and (31) for macroscopically inhomogeneous systems, are among the main results of the paper. It is worth emphasizing the frequency-space factorization of the correlator, which plays an important role in the theory of dephasing, cf. Sec. VII. The relation of Eq. (31) to the correlation function of the currents, Eq. (1), is discussed in Appendix B, and allows to put the presentation of the introduction on firm ground.

Note that Eq. (29) allows one to neglect the term Δ_x/κ^2 in Eq. (27) and thus reduce Eq. (27) to the form of the phenomenological integral equation (12), with U_{RPA} taking the place of Υ. [The same replacement leads from Eq. (11) to Eq. (20).] In other words, the electric potential of the fluctuating charge densities itself is negligible when screening is strong enough (i.e., good conductors in the unitary limit), justifying a *posteriori* our assumptions in the phenomenological Sec. II.

The fact that the correlation function of the potential is proportional to the solution of the diffusion equation at zero frequency, cf. Eq. (31), may be understood as a nonlocal version of the Johnson-Nyquist theorem, since $P(\boldsymbol{x},\boldsymbol{y},0)$ can be related to the classical dc resistance $\mathcal{R}(\boldsymbol{x},\boldsymbol{y})$ between the points $\boldsymbol{x}$ and $\boldsymbol{y}$ (see Ref. 20):

$$\mathcal{R}(\boldsymbol{x},\boldsymbol{y}) = \frac{2D}{\sigma_0}\left\{\frac{1}{2}[P(\boldsymbol{x},\boldsymbol{x},0) + P(\boldsymbol{y},\boldsymbol{y},0)] - P(\boldsymbol{x},\boldsymbol{y},0)\right\}. \tag{32}$$

For example, in an infinitely long quasi-1D wire of cross section s, the solution of the diffusion equation is $P(\boldsymbol{x},\boldsymbol{y},0) = -|x-y|/(Ds)$, where x is the component of $\boldsymbol{x}$ along the wire. Hence, we recover a resistance proportional to the distance between the points, $\mathcal{R}(\boldsymbol{x},\boldsymbol{y}) = |x-y|/(s\sigma_0)$.

VI. NOISE CORRELATION FUNCTION IN NETWORKS OF DISORDERED WIRES

Let us now illustrate the calculation of the noise correlation function, Eq. (31), for a network of disordered wires. The main ingredient to Eq. (31) is the solution of the diffusion equation (24) at zero frequency. Wires allow a quasi-1D description of diffusion, where transverse directions can be integrated out since $P(\boldsymbol{x},\boldsymbol{y},\omega)$ is assumed to be constant on the scale of the width of the wire. As a result, we replace $P(\boldsymbol{x},\boldsymbol{y},\omega) \to P(x,y,\omega)/s$, where s is the cross section of the wires and $P(x,y,\omega)$ solves the 1D diffusion equation in the network, x and y being coordinates along the wires. Recently, effective methods have been developed to solve the resulting diffusion equation for arbitrary networks.[10,20–22] We

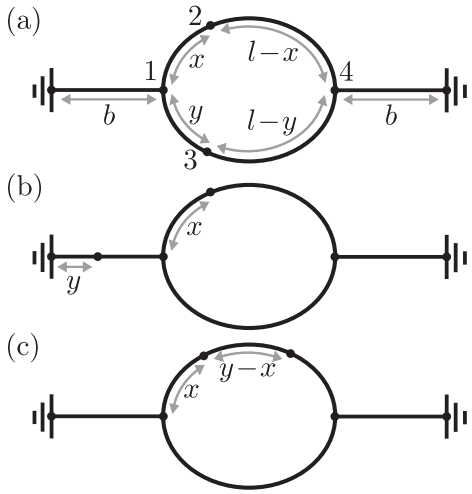

FIG. 5. The network corresponding to a symmetric ring made of four wires connected to two absorbing leads. The length of the arcs is l and the length of the connecting arms is b. Vertices are labeled by numbers $\alpha = 1,2,3,$ and 4. Vertices "1" and "4" denote the points where the ring is connected to the arms. Vertex "2" is always placed in the upper arc, defining the running coordinate x. Vertex "3" determines the y coordinate and is placed either in the adjacent arc (panel a) or in the left arc (panel b) or in the same arc (panel c).

will review these methods in this section and evaluate the noise correlation function for a simple example.

We start by introducing some basic notations: a network is a set of vertices, labeled by an index α, connected via wires of arbitrary length, say $l_{\alpha\beta}$ for the wire connecting vertices α and β. Let us define a vertex matrix $\mathcal{M}$ as

$$\mathcal{M}_{\alpha\beta} = \delta_{\alpha\beta} \sum_{\gamma} \frac{a_{\alpha\gamma}}{l_{\alpha\gamma}} - \frac{a_{\alpha\beta}}{l_{\alpha\beta}}, \tag{33}$$

where $a_{\alpha\beta} = 1$ if the vertices α and β are connected and $a_{\alpha\beta} = 0$ otherwise. The solution of the diffusion equation at zero frequency between arbitrary vertices α and β of the network is given by the entries of the inverse matrix $\mathcal{M}$ divided by the diffusion constant:

$$P(\alpha,\beta,0) = (\mathcal{M}^{-1})_{\alpha\beta}/D\,. \tag{34}$$

This allows us to calculate the noise correlation function between arbitrary points of a network by inserting vertices and inverting $\mathcal{M}$. As an aside, note that arbitrary boundary conditions can be included in this scheme easily (see Refs. 22 and 20 for details).

Let us consider the network shown in Fig. 5, representing a ring connected to absorbing leads. For simplicity, we assumed that the ring is symmetric: the two arcs are of the same length l and the connecting arms of length b. We evaluate the noise correlation function for two points in this network by inserting two vertices, called "2" and "3". Vertex 2 is always placed in the upper arc, encoding the running coordinate x in the length of the connected wires. Vertex 3 determines the y coordinate and is placed either in the lower arc or in the left connecting

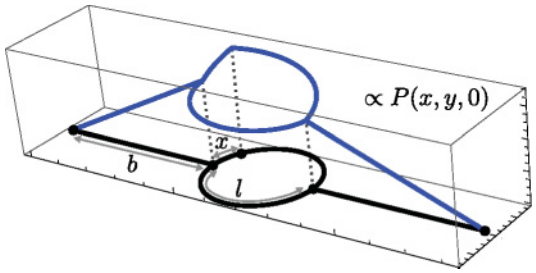

FIG. 6. (Color online) The solution to the diffusion equation at zero frequency, $P(x,y,0) \propto \langle|V|^2\rangle(x,y,\omega)\rangle$, where $\langle|V|^2\rangle$ is given by Eqs. (36)–(38), for a fixed coordinate x in the upper arm of the ring (indicated by the dot), as a function of y traversing the network. $\langle|V|^2\rangle(x,y,\omega)$ is linear in y and its derivative has a discontinuity at $y = x$.

arm or in the upper arc. In the first case, Fig. 5(a), the vertex matrix, Eq. (33), is given by

$$\mathcal{M} = \begin{pmatrix} \frac{1}{b}+\frac{1}{x}+\frac{1}{y} & -\frac{1}{x} & -\frac{1}{y} & 0 \\ -\frac{1}{x} & \frac{1}{x}+\frac{1}{l-x} & 0 & -\frac{1}{l-x} \\ -\frac{1}{y} & 0 & \frac{1}{y}+\frac{1}{l-y} & -\frac{1}{l-y} \\ 0 & -\frac{1}{l-x} & -\frac{1}{l-y} & \frac{1}{b}+\frac{1}{l-x}+\frac{1}{l-y} \end{pmatrix}. \tag{35}$$

The diffusion propagator is then given by $P(x,y,0) = (\mathcal{M}^{-1})_{23}/D$, and we obtain from Eq. (31) the correlation function as a function of the running coordinates x, $y \in [0,l]$:

$$\langle|V|^2\rangle(x,y,\omega) = \frac{\omega F(\omega)}{Dvs} \frac{b(l(2b+l) - (x+y)l + 2xy)}{l(4b+l)}. \tag{36}$$

When vertex 3 is placed in the connecting arm, $x \in [0,l]$ and $y \in [0,b]$ [Fig. 5(b)], we get

$$\langle|V|^2\rangle(x,y,\omega) = \frac{\omega F(\omega)}{Dvs} \frac{y(2b+l-x)}{4b+l}. \tag{37}$$

Finally, when vertex 3 is placed in the same arc of the ring as vertex 2 [see Fig. 5(c)], following the same logic we obtain, with $0 < x < y < l$,

$$\langle|V|^2\rangle(x,y,\omega) = \frac{\omega F(\omega)}{Dvs} \frac{bl(2b+l) + xl(3b+l) - ybl - xy(2b+l)}{l(4b+l)}. \tag{38}$$

All other configurations can be found by symmetry arguments. We plot $P(x,y,0)$ for y traversing the whole network in Fig. 6. Note that the resulting function is linear in y and its derivative has a discontinuity at $y = x$ (cf. Ref. 7).

VII. APPLICATION TO DEPHASING

The precise characterization of potential fluctuations is very important in studying phase coherent properties of disordered metals at low temperatures. To be specific, let us discuss a particular coherent property: the weak localization correction to the conductivity. Let us recall that the weak localization (WL) correction $\Delta\sigma \equiv \overline{\sigma} - \sigma_0$ is a small contribution to the

averaged conductivity arising from quantum interference of reversed diffusive electronic trajectories.[23]

At low temperatures, dephasing is dominated by electron interactions, that can be accounted for through a contribution to the phase accumulated by two time-reversed interfering trajectories in a fluctuating electric field[2]:

$$\Phi[\boldsymbol{x}(\tau)] = \int_0^t d\tau\ [V(\boldsymbol{x}(\tau),\tau) - V(\boldsymbol{x}(\tau),t-\tau)]. \quad (39)$$

When averaged over the Gaussian fluctuations of the electric field, $\langle e^{i\Phi}\rangle_V = e^{-\frac{1}{2}\langle\Phi^2\rangle_V}$ yields a phase difference that cuts off the contributions of long electronic trajectories. Introducing the trajectory- dependent dephasing rate $\Gamma[\boldsymbol{x}(\tau)] = \frac{1}{2t}\langle\Phi[\boldsymbol{x}(\tau)]^2\rangle_V$, the weak localization correction takes the form:[7,20,24,25]

$$\Delta\sigma(\boldsymbol{x}) = -\frac{2e^2D}{\pi}\int_0^\infty dt\ P(\boldsymbol{x},\boldsymbol{x},t)\,\langle e^{-t\Gamma[\boldsymbol{x}(\tau)]}\rangle_{\{\boldsymbol{x}(\tau)\}}, \quad (40)$$

where $\langle\cdots\rangle_{\{\boldsymbol{x}(\tau)\}}$ is the average with respect to closed diffusive trajectories of duration t starting from $\boldsymbol{x}$ (not to be confused with the thermal average $\langle\cdots\rangle_V$ over the electric potential V). The phase fluctuations can then be related to the potential fluctuations:

$$\frac{1}{2}\langle\Phi[\boldsymbol{x}]^2\rangle = \int_0^t d\tau d\tau'\int_{-\infty}^\infty \frac{d\omega}{2\pi}[e^{-i\omega(\tau-\tau')} - e^{-i\omega(\tau+\tau'-t)}] \times \langle|V|^2\rangle_\varphi(\boldsymbol{x}(\tau),\boldsymbol{x}(\tau',\omega). \quad (41)$$

Here, we have introduced a new noise correlator,

$$\langle|V|^2\rangle_\varphi(\boldsymbol{x},\boldsymbol{y},\omega) = \frac{1}{\nu}\,\omega F_\varphi(\omega)P(\boldsymbol{x},\boldsymbol{y},0), \quad (42)$$

obtained from Eq. (31) by replacing $F(\omega)$ with a modified function $F_\varphi(\omega)$ (given below), on the origin of which we now comment. Equation (20) is well-known in the theory of dephasing: its version symmetrized with respect to frequency arises naturally when comparing the diagrammatic calculation of the dephasing time[26,27] with the influence functional approach describing electrons moving in a random Gaussian field V.[24,28,29] Diagrammatically, the symmetrized Eq. (20) represents the Keldysh component of the screened-electron-interaction propagator, the only substantial difference being that the diagrammatically calculated correlation function involved in the dephasing process acquires so-called Pauli factors that account for the fact that the Fermi sea limits the phase space available for inelastic transitions.[28] These factors lead to the following replacement of the function $F(\omega)$ in Eq. (20) and also in Eq. (31):

$$F(\omega) \xrightarrow{\text{sym}} \coth(\omega/2T) \xrightarrow{\text{Pauli}} \frac{\omega/2T}{\sinh^2(\omega/2T)} \equiv F_\varphi(\omega). \quad (43)$$

This restricts the energy transfer to $|\omega| < T$,[24,27] but does not affect the factorization of the correlator. Inserting Eq. (42) into Eq. (41) leads to

$$\frac{1}{2}\langle\Phi[\boldsymbol{x}]^2\rangle = \frac{2T}{\nu}\int_0^t d\tau d\tau'\,P(\boldsymbol{x}(\tau),\boldsymbol{x}(\tau'),0)\int_{-\infty}^\infty\frac{d\omega}{2\pi} \times [e^{-i\omega(\tau-\tau')} - e^{-i\omega(\tau+\tau'-t)}]\frac{\omega}{2T}F_\varphi(\omega). \quad (44)$$

The fact that the frequency dependent function $\frac{\omega}{2T}F_\varphi(\omega)$ is symmetric allows us to add to $P(\boldsymbol{x}(\tau),\boldsymbol{x}(\tau'),0)$ the term $-\frac{1}{2}[P(\boldsymbol{x}(\tau),\boldsymbol{x}(\tau),0) + P(\boldsymbol{x}(\tau'),\boldsymbol{x}(\tau'),0)]$, which does not contribute to the integral (44). Therefore, we finally end up with the following expression for the dephasing rate,

$$\Gamma[\boldsymbol{x}(\tau)] = e^2T\int_0^t\frac{d\tau}{t}\int_0^t d\tau'\,[\delta_T(\tau+\tau'-t) - \delta_T(\tau-\tau')] \times \mathcal{R}(\boldsymbol{x}(\tau),\boldsymbol{x}(\tau')), \quad (45)$$

written in terms of the resistance $\mathcal{R}$, defined in Eq. (32). The function $\delta_T(t)$, a broadened delta function of width $1/T$ and height T, is the Fourier transform of $\frac{\omega}{2T}F_\varphi(\omega)$, which is given by

$$\delta_T(\tau) = \pi T\,w(\pi T\tau), \quad w(y) = \frac{y\coth y - 1}{\sinh^2 y}. \quad (46)$$

Equation (45), which is one of the main results of our paper, generalizes the results obtained in Refs. 8,9,24, and 28 for an infinite wire and an isolated ring to arbitrary geometry. In the classical noise limit $T\to\infty$, $\delta_T(\tau)$ may be replaced by a $\delta(\tau)$ function: the second term of Eq. (45) vanishes and we recover the results of Refs. 7 and 20.

Let us now illustrate Eq. (45) by calculating the dephasing time for the well-understood case of one and two-dimensional isolated simply-connected samples. The dephasing time can be extracted from the condition

$$1 \equiv \Gamma(\tau_\varphi)\tau_\varphi, \quad (47)$$

where $\Gamma(t)$ is given by the functional Eq. (45), averaged over the typical closed random walks $\boldsymbol{x}(\tau)$ of duration t in the system. The problem is governed by the interplay of three time scales: the Thouless time $\tau_{\rm Th} = L^2/D$, depending on the system size L, the thermal time $\tau_T = 1/T$ (related to the thermal length $L_T = \sqrt{D/T}$), and the dephasing time τ_φ.

(i) Diffusive regime, $\tau_T \ll \tau_\varphi \ll \tau_{\rm Th}$ ($L_T \ll L_\varphi \ll L$): this is the regime considered in Refs. 2 and 25, where the width of the broadened delta functions in Eq. (45), τ_T, is the shortest time scale. Thus, when averaging over paths $\boldsymbol{x}(\tau)$, the characteristic length scale $|x-y|$ entering the resistance $\mathcal{R}(x,y)$ can be determined as follows: for the first δ_T term, this length is governed by free diffusion, since $|\boldsymbol{x}(\tau) - \boldsymbol{x}(t-\tau)| \sim \sqrt{D\tau}$, hence $|x-y| \sim \sqrt{D\tau}$. For the second term, the characteristic length is set by the width of the delta function, $|x-y| \sim \sqrt{D\tau_T}$. In 1D, where $\mathcal{R}(x,y) \sim |x-y|/\sigma_0 s$, the first term dominates and we immediately obtain from Eq. (47) $1/\tau_\varphi \sim (e^2\sqrt{D}T/\sigma_0 s)^{2/3}$. In 2D, the diffuson at zero frequency is logarithmic as well as the resistance (32), $\mathcal{R}(x,y) \sim \ln(|x-y|)/\sigma_0 d$, where d is the width of the sample, which can be understood from the fact that the resistance of a plane connected at two corners scales logarithmically with the system size. Equation (47) gives $1 \sim e^2T\tau_\varphi\ln(T\tau_\varphi)/\sigma_0 d$, and for the dephasing time, $1/\tau_\varphi \sim e^2T\ln(e^2/\sigma_0 d)/\sigma_0 d$.

(ii) Ergodic regime, $\tau_T \ll \tau_{\rm Th} \ll \tau_\varphi$ ($L_T \ll L \ll L_\varphi$): the width of $\delta_T(\tau)$ in Eq. (45) is still the shortest time scale but, in contrast to (i), the typical trajectories $\boldsymbol{x}(\tau)$ explore the whole system, setting the length scale of diffusion to the system size L, cf. Refs. 6 and 7. In full analogy to the diffusive regime, but replacing $\sqrt{D\tau}$ by L, we find for 1D, $1/\tau_\varphi \sim e^2LT/\sigma_0 s$, and for 2D, $1/\tau_\varphi \sim e^2T\ln(\tau_{\rm Th}/\tau_T)/\sigma_0 d$.[30] These examples show that for nontrivial geometries, dephasing due to electron interactions cannot be accounted for through

a unique dephasing rate depending only on dimensionality, but must be described by a functional of the trajectories $\boldsymbol{x}(\tau)$ since the qualitative behavior of τ_φ follows from the geometry dependent typical distance $|\boldsymbol{x}(\tau)-\boldsymbol{x}(\tau')|$.

For sufficiently low temperatures, on the other hand, Eq. (45) is capable to describe the crossover to a 0D regime, where, apart from a dependence on the total system size, geometry becomes unimportant.

(iii) 0D regime, $\tau_{\rm Th} \ll \tau_T \ll \tau_\varphi$ ($L \ll L_T \ll L_\varphi$): here, the width of the delta functions in Eq. (45), τ_T, is larger than $\tau_{\rm Th}$. Hence, the trajectories reach the ergodic limit $\boldsymbol{x}(\tau \geqslant \tau_{\rm Th}) \sim L$ before the electric potential has significantly changed: dephasing is strongly reduced. Let us denote the maximal resistance reached at the ergodic limit as $\mathcal{R}_{\rm erg}$ and replace the resistance in Eq. (45) by $\mathcal{R} \to \mathcal{R} - \mathcal{R}_{\rm erg}$, without changing the result, since $\mathcal{R}_{\rm erg}$ is constant and its contribution vanishes after integrating over τ and τ'. The difference $\mathcal{R} - \mathcal{R}_{\rm erg}$ is nonzero only during time differences $\tau - \tau' \lesssim \tau_{\rm Th}$ before reaching ergodicity. Thus the leading contribution comes from the second δ_T term in Eq. (45), which is constant at its maximum T during such short time scales. We find $1 \sim -e^2T^2\tau_\varphi \int_0^{\tau_{\rm Th}} d\tau\, [\mathcal{R}(\boldsymbol{x}(\tau),0) - \mathcal{R}_{\rm erg}]$ and since the $\mathcal{R}_{\rm erg}$ term dominates, we obtain a dephasing time $1/\tau_\varphi \sim e^2T^2\tau_{\rm Th}\mathcal{R}_{\rm erg}$, independent of geometry and with the characteristic $\sim T^2$ behavior.[31]

VIII. CONCLUSIONS

In this paper, we have considered fluctuations of the scalar electric potentials in macroscopically inhomogeneous metals. We have shown how to relate the density fluctuations to the potential fluctuations, emphasizing the role of electronic interactions, provided a real space derivation of the density response function, and illustrated these general ideas for the case of networks of metallic wires. Finally, we have obtained a trajectory-dependent functional, Eq. (45), which describes dephasing by electron interactions for arbitrary geometries and accounts for the quantum noise contribution. When applied to networks, Eq. (45) can describe the full crossover from the 0D to the 1D and the 2D regime.

ACKNOWLEDGMENTS

We acknowledge illuminating discussions with F. Marquardt and support from the DFG through SFB TR-12 (O. Ye.), DE 730/8-1 (M. T.) and the Cluster of Excellence, Nanosystems Initiative, Munich.

APPENDIX A: SELF CONSISTENT ANALYSIS OF SCREENING

We recall here how to obtain Eq. (17) using a self-consistent treatment of screening in real space.[32] Starting points are the following three equations: (i) the excess charge density is decomposed into external and induced contributions

$$\delta n(\boldsymbol{x},\omega) = n_{\rm ext}(\boldsymbol{x},\omega) + n_{\rm ind}(\boldsymbol{x},\omega). \tag{A1}$$

(ii) The induced charge is related to the potential $V(\boldsymbol{x},\omega)$ by the density response function, cf. Eq. (4):

$$n_{\rm ind}(\boldsymbol{x},\omega) = -\int d\boldsymbol{y}\ \chi(\boldsymbol{x},\boldsymbol{y},\omega)\, V(\boldsymbol{y},\omega). \tag{A2}$$

(iii) The Poisson equation

$$\Delta\, V(\boldsymbol{x},\omega) = -4\pi e^2\, \delta n(\boldsymbol{x},\omega). \tag{A3}$$

Self-consistency lies in the fact that the response involves the screened potential $V(\boldsymbol{x},\omega)$ and not the bare "external" potential related to $n_{\rm ext}(\boldsymbol{x},\omega)$. The screened effective interaction between electrons $U_{\rm RPA}(\boldsymbol{x},\boldsymbol{y},\omega)$ is obtained by placing an external charge at $\boldsymbol{y}$, so that the external density is $n_{\rm ext}(\boldsymbol{x},\omega) = \delta(\boldsymbol{x}-\boldsymbol{y})$, and associating the resulting screened potential $V(\boldsymbol{x},\omega)$ in Eq. (A3) with $U_{\rm RPA}(\boldsymbol{x},\boldsymbol{y},\omega)$. We obtain

$$-\frac{1}{4\pi e^2}\Delta_x U_{\rm RPA}(\boldsymbol{x},\boldsymbol{y},\omega) + \int d\boldsymbol{x}'\ \chi(\boldsymbol{x},\boldsymbol{x}',\omega) U_{\rm RPA}(\boldsymbol{x}',\boldsymbol{y},\omega) = \delta(\boldsymbol{x}-\boldsymbol{y}). \tag{A4}$$

Convolution with the Coulomb interaction gives Eq. (17).

APPENDIX B: CURRENT DENSITY CORRELATIONS

We discuss here the relation between the density and the current density correlations. The response of the (induced) current density is characterized by the conductivity tensor σ,

$$\langle \hat{j}_\alpha(\boldsymbol{x},\omega)\rangle_{\rm neq} = \int d\boldsymbol{y}\, \sigma_{\alpha\beta}(\boldsymbol{x},\boldsymbol{y},\omega)\, E_\beta(\boldsymbol{y},\omega), \tag{B1}$$

which is related to Eq. (5) by current conservation:

$$\nabla_\alpha \nabla'_\beta \sigma_{\alpha\beta}(\boldsymbol{x},\boldsymbol{x}',\omega) = -i\omega e^2 \chi(\boldsymbol{x},\boldsymbol{x}',\omega). \tag{B2}$$

The thermal fluctuations of the current density can be obtained from $\langle j_\alpha j_\beta^\dagger\rangle(\boldsymbol{x},\boldsymbol{y},\omega) = \omega F(\omega)\,{\rm Re}[\sigma_{\alpha\beta}(\boldsymbol{x},\boldsymbol{y},\omega)]$, in analogy to the discussion in Sec. II, assuming time-reversal symmetry, $\sigma_{\alpha\beta}(\boldsymbol{x},\boldsymbol{y},\omega) = \sigma_{\beta\alpha}(\boldsymbol{y},\boldsymbol{x},\omega)$.

Let us now examine the case of disordered metals. The classical contribution to the averaged nonlocal dc conductivity has been derived in Ref. 12. Their result can be generalized straightforwardly to nonzero frequencies,

$$\overline{\sigma}_{\alpha\beta}(\boldsymbol{x},\boldsymbol{x}',\omega) = \sigma_0\,[\delta_{\alpha\beta}\delta(\boldsymbol{x}-\boldsymbol{x}') - D\nabla_\alpha\nabla'_\beta P(\boldsymbol{x},\boldsymbol{x}',\omega)], \tag{B3}$$

which obeys the condition (B2) with Eq. (25) substituted for χ. For the current correlations, we find[33]

$$\overline{\langle j_\alpha j_\beta^\dagger\rangle}(\boldsymbol{x},\boldsymbol{x}',\omega) = \sigma_0\,\omega F(\omega)\,\{\delta_{\alpha\beta}\delta(\boldsymbol{x}-\boldsymbol{x}') - D\nabla_\alpha\nabla'_\beta {\rm Re}[P(\boldsymbol{x},\boldsymbol{x}',\omega)]\}. \tag{B4}$$

Since the diffuson $P(\boldsymbol{x},\boldsymbol{x}',\omega)$ decays exponentially on a length scale $L_\omega = \sqrt{D/\omega}$, this expression shows that current correlations can be considered as purely local over the scale $||\boldsymbol{x}-\boldsymbol{x}'|| \gg L_\omega$, i.e., $\overline{\langle|j|^2\rangle}(\boldsymbol{x},\boldsymbol{x}',\omega) \simeq \sigma_0\omega F(\omega)\delta(\boldsymbol{x}-\boldsymbol{x}')$. In the limit of classical noise, $F(\omega)\,\omega \simeq 2T$, we recover precisely Eq. (1).

[1]J. B. Johnson, Phys. Rev. **32**, 97 (1928); H. Nyquist, *ibid.* **32**, 110 (1928).
[2]B. L. Altshuler, A. G. Aronov, and D. E. Khmelnitsky, J. Phys. C **15**, 7367 (1982).
[3]M. Ferrier, L. Angers, A. C. H. Rowe, S. Guéron, H. Bouchiat, C. Texier, G. Montambaux, and D. Mailly, Phys. Rev. Lett. **93**, 246804 (2004).
[4]F. Schopfer, F. Mallet, D. Mailly, C. Texier, G. Montambaux, C. Bäuerle, and L. Saminadayar, Phys. Rev. Lett. **98**, 026807 (2007).
[5]M. Ferrier, A. C. H. Rowe, S. Gueron, H. Bouchiat, C. Texier, and G. Montambaux, Phys. Rev. Lett. **100**, 146802 (2008).
[6]T. Ludwig and A. D. Mirlin, Phys. Rev. B **69**, 193306 (2004).
[7]C. Texier and G. Montambaux, Phys. Rev. B **72**, 115327 (2005).
[8]M. Treiber, O. M. Yevtushenko, F. Marquardt, J. von Delft, and I. V. Lerner, Phys. Rev. B **80**, 201305(R) (2009).
[9]M. Treiber, O. M. Yevtushenko, F. Marquardt, J. von Delft, and I. V. Lerner, in *Perspectives of Mesoscopic Physics: Dedicated to Yoseph Imry's 70th Birthday*, edited by A. Aharony, O. Entin-Wohlman (World Scientific, Singapore, 2010), Chap. 20.
[10]C. Texier and G. Montambaux, Phys. Rev. Lett. **92**, 186801 (2004).
[11]A. Yu. Zyuzin and B. Z. Spivak, Sov. Phys. JETP **66**, 560 (1987); [Zh. Eksp. Teor. Fiz. **93**, 994 (1987)].
[12]C. L. Kane, R. A. Serota, and P. A. Lee, Phys. Rev. B **37**, 6701 (1988).
[13]I. V. Lerner, Sov. Phys. JETP **68**, 143 (1989) [Zh. Eksp. Teor. Fiz. **95**, 253 (1989)].
[14]L. D. Landau and E. M. Lifshitz, *Statistical Physics*, 3rd ed. (Butterworth-Heinemann, 1980), Vol. 5.
[15]In general, if the electromagnetic field is not quantized, as is the case here, the potential is not an operator; the assumption of a potential operator arises from electronic interactions that relate the internal electronic density operator to the electric potential.
[16]The different signs in Eqs. (7) and (11) reflect the different sign conventions in Eqs. (4) and (10).
[17]D. Vollhardt and P. Wölfle, Phys. Rev. B **22**, 4666 (1980).
[18]E. Akkermans and G. Montambaux, *Mesoscopic Physics of Electrons and Photons* (Cambridge University Press, Cambridge, 2007).
[19]R. P. Kanwal, *Linear Integral Equations: Theory & Technique* (Birkenhäuser, Boston, 1997).
[20]C. Texier, P. Delplace, and G. Montambaux, Phys. Rev. B **80**, 205413 (2009).
[21]M. Pascaud and G. Montambaux, Phys. Rev. Lett. **82**, 4512 (1999).
[22]E. Akkermans, A. Comtet, J. Desbois, G. Montambaux, and C. Texier, Ann. Phys. (NY) **284**, 10 (2000).
[23]D. E. Khmelnitskii, Physica B & C **126**, 235 (1984).
[24]F. Marquardt, J. von Delft, R. Smith, and V. Ambegaokar, Phys. Rev. B **76**, 195331 (2007).
[25]G. Montambaux and E. Akkermans, Phys. Rev. Lett. **95**, 016403 (2005).
[26]I. L. Aleiner, B. L. Altshuler, and M. E. Gershenson, Waves in Random and Complex Media **9**, 201 (1999).
[27]J. von Delft, F. Marquardt, R. Smith, and V. Ambegaokar, Phys. Rev. B **76**, 195332 (2007).
[28]J. von Delft, Int. J. Mod. Phys. B **22**, 727 (2008).
[29]S. Chakravarty and A. Schmid, Phys. Rep. **140**, 193 (1986).
[30]Compare with Y. Takane, *Anomalous Behavior of the Dephasing Time in Open Diffusive Cavities*, J. Phys. Soc. Jpn. **72**, 233 (2003), where vertex diagrams[27,28] have not been considered.
[31]U. Sivan, Y. Imry, and A. G. Aronov, Europhys. Lett. **28**, 115 (1994).
[32]T. Christen and M. Büttiker, Europhys. Lett. **35**, 523 (1996).
[33]Note that the FDT expresses thermal correlations $\overline{\langle \boldsymbol{j}^2\rangle(\boldsymbol{x},\boldsymbol{y},\omega)} \equiv \overline{\langle j(\boldsymbol{x},\omega)j(\boldsymbol{y},-\omega)\rangle} \sim \mathrm{Re}[\overline{\sigma}(\boldsymbol{x},\boldsymbol{y},\omega)]$, dominated by short-range contributions; this should not be confused with the mesoscopic correlations $\overline{\langle j(\boldsymbol{x},\omega)\rangle\langle j(\boldsymbol{x}',\omega')\rangle} \sim \overline{\sigma(\boldsymbol{x},\boldsymbol{y},\omega)\sigma(\boldsymbol{x}',\boldsymbol{y}',\omega')}$ studied in Refs. 11–13, dominated by long-range contributions.